



# Evaluation of the anti-diabetic drug sitagliptin as a novel attenuate to SARS-CoV-2 evidence-based in silico: molecular docking and molecular dynamics

José Ednésio da Cruz Freire<sup>1,2,3</sup> · José Edvar Monteiro Júnior<sup>4</sup> · Daniel Pascoalino Pinheiro<sup>5</sup> · Grayce Ellen da Cruz Paiva Lima<sup>1,2,3,6</sup> · Camila Lopes do Amaral<sup>1,2,3</sup> · Víctor Rezende Veras<sup>1,2</sup> · Mayara Ponte Madeira<sup>1,2,3,7</sup> · Erika Bastos Lima Freire<sup>1,2,3,7</sup> · Renan Galvão Ozório<sup>1,2</sup> · Virgínia Oliveira Fernandes<sup>1,2,3,8</sup> · Ana Paula Dias Rangel Montenegro<sup>1</sup> · Raquel Carvalho Montenegro<sup>2</sup> · Jeová Keny Baima Colares<sup>3</sup> · Renan Magalhães Montenegro Júnior<sup>1,2,3,8</sup>

Received: 30 July 2022 / Accepted: 30 September 2022  
© King Abdulaziz City for Science and Technology 2022

## Abstract

The current outbreak of COVID-19 cases worldwide has been responsible for a significant number of deaths, especially in hospitalized patients suffering from comorbidities, such as obesity, diabetes, hypertension. The disease not only has prompted an interest in the pathophysiology, but also it has propelled a massive race to find new anti-SARS-CoV-2 drugs. In this scenario, known drugs commonly used to treat other diseases have been suggested as alternative or complementary therapeutics. Herein we propose the use of sitagliptin, an inhibitor of dipeptidyl peptidase-4 (DPP<sub>4</sub>) used to treat type-II diabetes, as an agent to block and inhibit the activity of two proteases, 3CL<sup>pro</sup> and PL<sup>pro</sup>, related to the processing of SARS-CoV-2 structural proteins. Inhibition of these proteases may possibly reduce the viral load and infection on the host by hampering the synthesis of new viruses, thus promoting a better outcome. In silico assays consisting in the modeling of the ligand sitagliptin and evaluation of its capacity to interact with 3CL<sup>pro</sup> and PL<sup>pro</sup> through the prediction of the ligand bioactivity, molecular docking, overlapping of crystal structures, and molecular dynamic simulations were conducted. The experiments indicate that sitagliptin can interact and bind to both targets. However, this interaction seems to be stronger and more stable to 3CL<sup>pro</sup> ( $\Delta G = -7.8 \text{ kcal mol}^{-1}$ ), when compared to PL<sup>pro</sup> ( $\Delta G = -7.5 \text{ kcal mol}^{-1}$ ). This study suggests that sitagliptin may be suitable to treat COVID-19 patients, beyond its common use as an anti-diabetic medication. In vivo studies may further support this hypothesis.

**Keywords** COVID-19 · DPP<sub>4</sub> · Sitagliptin · 3CL<sup>pro</sup> · PL<sup>pro</sup> · Anti-SARS-CoV-2

## Introduction

The 2019 coronavirus disease (COVID-19) was first reported in Wuhan, China, and it is caused by a novel  $\beta$ -*Coronavirus*, a zoonotic emerging pathogen identified in 2019. Systemic complications associated with COVID-19 disease, usually involve gastrointestinal infections, renal injury, heart failure (Amaral et al. 2022), leading to a relatively high mortality rate. Since the clinical manifestations of this disease resemble those caused by the classic SARS-CoV virus, the new

pathogen was named SARS-CoV-2. COVID-19 has been reported as the most devastating outbreak known to humans to date being responsible (Singh et al. 2021, 2022), only in Brazil, for a total of 683,965 deaths (<https://covid.saude.gov.br/>), until August 2022.

All CoVs are featured by a positive single-stranded RNA (Freire et al. 2020), and the increased lethality of this group is partly related to the presence of a high mutation rate due to their propensity to errors during the replication. In addition, it has been shown that during the infection, a mixture of different CoVs viral strains commonly causes an RNA homologous recombination of around 20% (Denison et al. 2011), which is assumed to explain the high tropism and pathogenicity the virus presents to the host (Cui et al. 2019).

✉ José Ednésio da Cruz Freire  
jednesio@gmail.com

Extended author information available on the last page of the article

Most CoVs, including SARS-CoV-2, use the C-terminal domain (CTD) of S<sub>1</sub> subunit of the glycoprotein spike to bind to the angiotensin-converting enzyme 2 (ACE<sub>2</sub>). The high affinity of the CTD to ACE<sub>2</sub> induces the virus-cell fusion (Huang et al. 2020) that later may result in serious organic disorders or death. SARS-CoV-2 is also capable to bind and interact with the transmembrane protease DPP<sub>4</sub>/CD<sub>26</sub> (dipeptidyl peptidase 4), and this has been proposed as an alternative pathway the virus may use to enter the host cell (Li et al. 2020). DPP<sub>4</sub> functions as a chemical modulator for several other molecules, such as cytokines, chemokines and growth factors, and some studies have reported that a high incidence of mortality and complications in diabetic patients suffering from MERS-CoV (a virus similar to SARS-CoV-2) infection may be related to dysregulated immune responses mediated by the DPP<sub>4</sub> (Li et al. 2017; Fan et al. 2018).

Gliptins are a class of oral antihyperglycemic agents with demonstrated efficacy in the treatment of type-II diabetes (Scheen 2013) acting as DPP<sub>4</sub> inhibitors (iDPP<sub>4</sub>). Sitagliptin is a member of the gliptin family that beyond its anti-diabetic effects presents low cardiovascular risks (Green et al. 2015; Yoshikawa et al. 2020). Considering that DPP<sub>4</sub> is an additional receptor which SARS-CoV-2 may recognize to enter the host cells, we propose that an iDPP<sub>4</sub>, as sitagliptin, may act as an antiviral drug. In fact, a recent paper has shown that sitagliptin significantly reduced SARS-CoV-2 titer in cell culture supernatants from infected cells (Narayanan et al. 2022).

Once inside the cell SARS-CoV-2 uses two key proteases, a chymotrypsin-like protease (3CL<sup>pro</sup>), and a papain-like protease (PL<sup>pro</sup>), to process the precursors of its 16 non-structural proteins (NSPs) (Yilmaz et al. 2020; Ravi et al. 2022; Yavarian et al. 2022), by a cascade of cleavage process as schematized in Fig. 1. Thus, the roles of 3CL<sup>pro</sup> and PL<sup>pro</sup> are of critical importance to the successful of the viral infection, making these proteases important targets to antiviral drugs addressing to SARS-CoV-2.

The discovery and development of drugs against any disease or a target is a cumbersome and time-demanding task. On the other hand, as observed in several cases around the world, many clinical professionals have reported the use of the repositioning approach (off label treatment) to treat COVID-19 patients (Abd-Elsalam et al. 2021; Kashour et al. 2021; Amaral et al. 2022); therefore, the aim of this work was to carry out a detailed in silico analysis to evaluate the potential of the molecule sitagliptin as bifunctional candidate to be used as a new anti-SARS-CoV-2 drug targeting not only the human DPP<sub>4</sub>, but also the 3CL<sup>pro</sup> and PL<sup>pro</sup> SARS-CoV-2 proteases.

## Methods

### Domain analysis and linker prediction of the target receptors

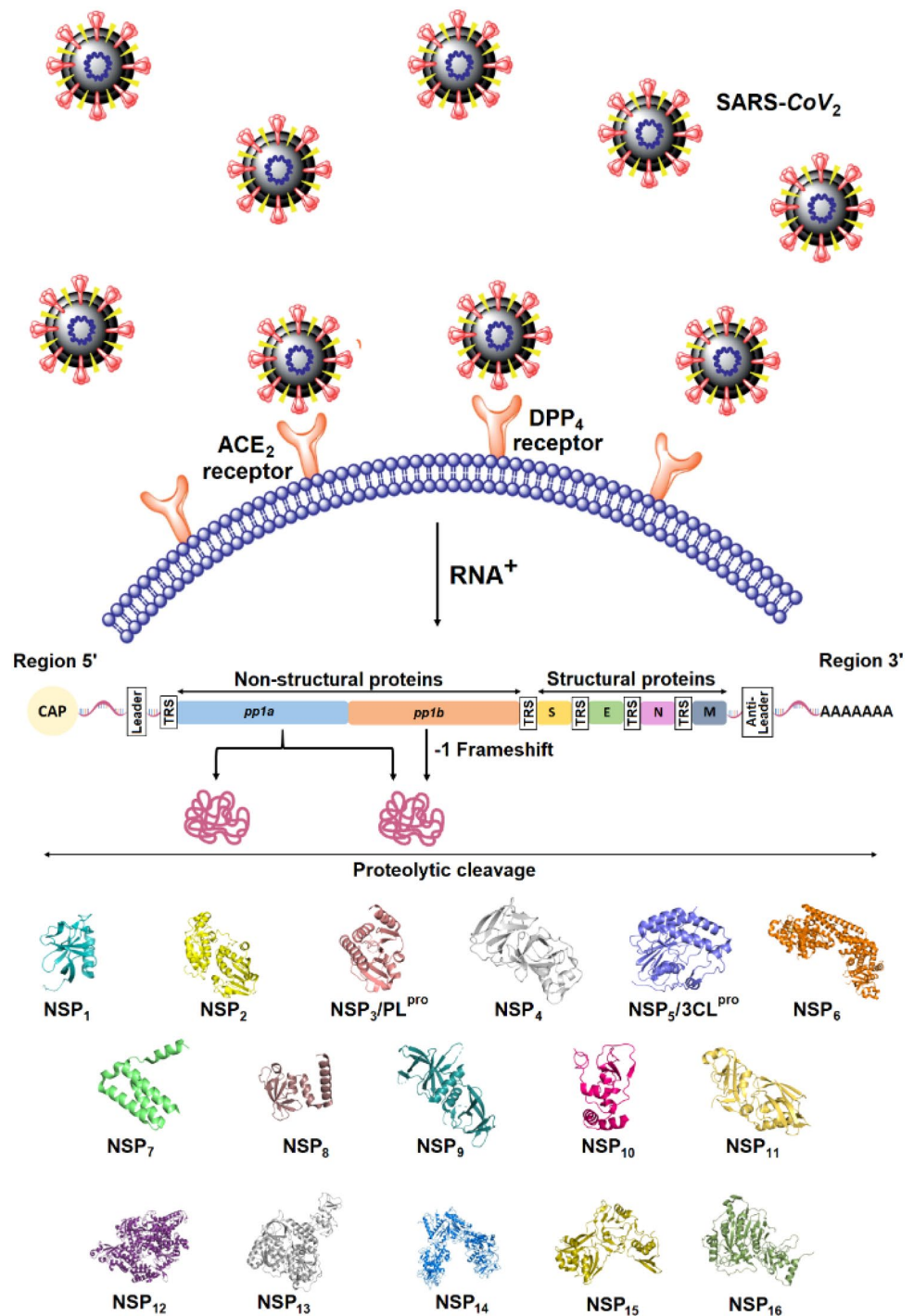
The structures and amino acid sequences of the papain-like protease PL<sup>pro</sup> from SARS-CoV (Ratia et al. 2006) and chymotrypsin-like protease - 3CL<sup>pro</sup> (Su et al. 2020) from SARS-CoV-2 (Accession PDB IDs: 2FE8 and 6M2N, respectively) were downloaded in *pdb* and *fasta* formats from the Protein Data Bank (Burley et al. 2021). In order to identify possible boundary domains as well as to predict linker sequences, the amino acids sequences of PL<sup>pro</sup> and 3CL<sup>pro</sup> were submitted to the following servers: Database of Protein Domains, Families and Functional Sites - Prosite (Sigrist et al. 2012), Conserved Domains Database and Resources - CDD (Lu et al. 2020), and Classification of Protein Families - InterPro (Blum et al. 2021). The algorithms employed by FTSite (Ngan et al. 2012), FTMap (Kozakov et al. 2015), and CASTp (Tian et al. 2018) servers were used to identify the interaction regions (hotspots).

### Ligand design, bioactivity prediction, and molecular docking studies

The structure of the ligand (sitagliptin) was designed with the software MarvinSketch 6.2.2 (ChemAxon - <http://www.chemaxon.com/products/marvin/marvinsketch/>). The output file was submitted to Molinspiration Virtual Screening ([www.molinspiration.com](http://www.molinspiration.com)) and ChEMBL (Mendez et al. 2019) servers to calculate the molecular properties and bioactivity score of sitagliptin.

Docking simulations were conducted with the AutoDock Vina software v. 1.1.2 (Trott and Olson 2010). Initially, in order to validate our molecular docking, site-directed redocking simulations were carried out under conditions where all the torsion connections of the ligand and amino acids present in the catalytic site of the receptor were free to rotate. All hydrogen polar atoms were previously added to the receptor and then parameterized with Gasteiger charges. The ligand was prepared by addition of Kollman charges. The simulation has been performed in the following conditions: number of conformations = 50, exhaustiveness = 33, and seed = 1000. The dimensions of the boxes in all cases were: X = 58 Å, Y = 80 Å, and Z = 62 Å. The crystal structure (PDB ID: 6M2N) of 3CL<sup>pro</sup> co-crystallized with the ligand baicalein was used for this challenge. Afterward, simulations employing the same strategy were performed using the ligand and the crystal structures of both the PL<sup>pro</sup> and 3CL<sup>pro</sup> as targets. Predictions made by CASTp, FTMap, and FTSite servers

**Fig. 1** Synthesis of non-structural proteins (NSPs) and post-translational modification mechanisms of SARS-CoV-2 virus. Stage 1: after recognition of the ACE<sub>2</sub> and/or DPP<sub>4</sub> cell receptors, the viral nucleocapsid is released into the cytoplasm by endocytosis, or fusion of the viral envelope, with the cell membrane. Stage 2: the translation of the *pp1a* and *pp1b* genes results in the synthesis of pp1a or pp1ab polyproteins, the latter being generated by a -1 frameshift of ribosomes. These polyproteins are then cleaved by viral 3CL<sup>pro</sup> and PL<sup>pro</sup> proteases generating 16 virus NSPs, including the RNA-dependent RNA polymerase (RdRp or NSP<sub>12</sub>)



were also used to determine the selected sites in PL<sup>pro</sup> and 3CL<sup>pro</sup> proteases for the molecular docking simulations.

All torsional bonds of the ligand (sitagliptin) were free to rotate, whereas the PL<sup>pro</sup> protease was held rigid except for the amino acids Trp<sup>107</sup>, Asp<sup>109</sup>, Cys<sup>112</sup>, Tyr<sup>113</sup>, Cys<sup>163</sup>, Gly<sup>164</sup>, Tyr<sup>265</sup>, Tyr<sup>269</sup>, Gln<sup>270</sup>, Cys<sup>271</sup>, His<sup>273</sup>, Tyr<sup>274</sup>, and Asp<sup>287</sup>. Similarly, the amino acids from 3CL<sup>pro</sup> protease

(Thr<sup>25</sup>, Thr<sup>26</sup>, Leu<sup>27</sup>, Arg<sup>40</sup>, His<sup>41</sup>, Val<sup>42</sup>, Ser<sup>46</sup>, Met<sup>49</sup>, Asn<sup>142</sup>, Gly<sup>143</sup>, Ser<sup>144</sup>, Cys<sup>145</sup>, His<sup>163</sup>, His<sup>164</sup>, Glu<sup>166</sup>, and Gln<sup>189</sup>) were kept free to rotate. The following coordinates:  $X = -20.941$ ,  $Y = 50.041$ , and  $Z = -2.974$  to the PL<sup>pro</sup>, and  $X = 115.371$ ,  $Y = -17.804$ , and  $Z = 62.399$  to the 3CL<sup>pro</sup> were used based on the predicted hotspots.

## Molecular dynamics simulation and schematic representations

Sitagliptin-PL<sup>PRO</sup> and sitagliptin-3CL<sup>PRO</sup> complexes presenting the lowest binding energy according to docking simulations were submitted to stability tests by MD analysis using the GROMACS package, version 2019.5 (Abraham et al. 2015). The electroneutrality of both complexes was maintained by adding Na<sup>+</sup> ions in the required amounts. System solvation was conducted using SPC/E (extended simple point charge model) water molecules in a periodic box (90×90×90 nm<sup>3</sup> volume) containing buffer to enable substantial fluctuations of the conformation during MD simulations. MD simulations were performed using the GROMOS 54a7 force field, a force field recently developed from three previous force fields (GROMOS 45A3, 53A6, and 54A7), and validated to simulate the folding equilibrium of  $\beta$ -peptides (as in the case of sitagliptin). The energy minimization (2000 steps steepest descent followed by 200-ps-long MD simulation) was performed before initiating MD simulations to remove initial steric clashes. MD simulations were performed under constant pressure using anisotropic diagonal position scaling with a time step of 0.002 ps. The electrostatic interactions were assessed based on the principle of PME (Particle Mesh Ewald) previously defined with short-range cutoffs of 1.2 nm (Essmann et al. 1995). The temperature of the system was parameterized to gradually increase from 100 up to 310 K at 1 bar pressure in 1000 ps. The Berendsen weak-coupling algorithm (Berendsen et al. 1984) with a constant time of 0.2 ps was used. The LINCS algorithm (Hess 2008) was used to constrain the equilibrium distances between all bonds allowing only internal motions of bending and torsion during MD simulations. Finally, the 25-ns MD simulations were performed under the same conditions as the equilibration procedure.

Two-dimensional representations of the best ligand–protein complexes based on the theoretical binding energy value were generated using the ProteinsPlus server (Schöning-Stierand et al. 2020). The software PyMol Molecular Graphics System, version 1.7.4 (Schrodinger, LLC), and the Protein–Ligand Interaction Profiler server (Adasme et al. 2021) were used to build the three-dimensional structures.

## Results

### Domain analysis and linker prediction of the target receptors

CDD-based annotation data showed that PL<sup>PRO</sup> belongs to the conserved protein domain family CoV-NSP<sub>3</sub>, also called  $\beta$ -*Coronavirus* non-structural protein 3, whereas 3CL<sup>PRO</sup> is a member of the conserved protein domain family

CoV-NSP<sub>5</sub>-M<sup>PRO</sup>, also called  $\beta$ -*Coronavirus* non-structural protein 5, or Main protease (M<sup>PRO</sup>). The analyses of the CDD-based annotation to PL<sup>PRO</sup> and 3CL<sup>PRO</sup> showed predictions with confidence indices in accordance with data previously presented: *E*-value (208<sup>-177</sup>, and 0<sup>00</sup>), Bit-Score (492.10, and 565.11), and interval (4 to 306, and 4 to 300 amino acids residues), respectively. All data reported above are in agreement with the predictions obtained by Prosite and InterPro servers. Mapping based of binding hotspots data showed that PL<sup>PRO</sup> presents only one organic probe cluster (site<sup>1</sup>), whereas for the 3CL<sup>PRO</sup> the results suggest the existence of four organic probe clusters (site<sup>1</sup>, site<sup>2</sup>, site<sup>3</sup>, and site<sup>4</sup>). The position of the interaction sites on both receptors identified here (PL<sup>PRO</sup> and 3CL<sup>PRO</sup>) did not differ from those previously reported (Abdizadeh et al. 2022; Zhao et al. 2022).

### Ligand bioactivity prediction

In silico predictions of sitagliptin bioactivity using Molinspiration Virtual Screening provided a score of 0.56, suggesting that this ligand can inhibit a broad range of proteases. In addition, the analysis returned a score of 0.25 which suggests that sitagliptin can bind to the G protein-coupled receptors (GPCR), while presented a reduced inhibitory activity against kinases, score of 0.01. The bioactivity of the whole ligand is predicted as the sum of the bioactivity scores of all individual fragments (a number typically ranging from -3 to 3). The results obtained from the ChEMBL server, indicated a significant pharmacological activity against the human DPP<sub>4</sub>, as indicated by confidence score values of 70%, 80%, and 90%, with a threshold value of 6. Furthermore, the analyses also suggested a probable interaction between sitagliptin and the viral proteins: *Human Immunodeficiency virus* - 1 integrase, and the RNA-dependent RNA polymerase from *Hepatitis C virus* NS<sub>5B</sub>, as showed by a confidence score value of 90%, also determined by a threshold value of 6 (Table 1).

## Molecular docking studies and Molecular Dynamics

### Molecular docking and molecular dynamics study: PL<sup>PRO</sup> and 3CL<sup>PRO</sup> proteases and the ligand sitagliptin

A total of 20 simulations (molecular docking) were performed for both systems: PL<sup>PRO</sup>-sitagliptin and 3CL<sup>PRO</sup>-sitagliptin. Molecular docking experiments for PL<sup>PRO</sup>-sitagliptin and 3CL<sup>PRO</sup>-sitagliptin returned best performance  $\Delta G = -7.5$  and  $\Delta G = -7.8$  kcal mol<sup>-1</sup>, respectively. It is important to note that  $\Delta G$  values represent the combined result of the van der Waals dispersive and electrostatic interaction energy which indicates the approximate binding energy between ligand and receptor.



**Table 1** The table shows ChEMBL targets which are predicted to interact with sitagliptin (ChEMBL<sub>1422</sub>)

Target protein	Source	Conf. 70%	Conf. 80%	Conf. 90%	Activity threshold
Dipeptidyl peptidase IV	<i>Homo sapiens</i>	Active	Active	Active	6
Integrase	<i>Human immunodeficiency virus - 1</i>	Empty	Empty	Active	6
RNA-dependent RNA polymerase	<i>Hepatitis C virus</i>	Empty	Empty	Active	6

The target prediction returns four classes: 'active' or 'inactive' depending on whether the ligand is predicted to interact or not with the target. The value returned can also be 'empty' if the model was not able to predict the compound or 'both' if it could not conclude. The predictions are given at three different confidence levels. More information on the methodology is available at: <https://jcheminf.biomedcentral.com/articles/10.1186/s13321-018-0325-4>

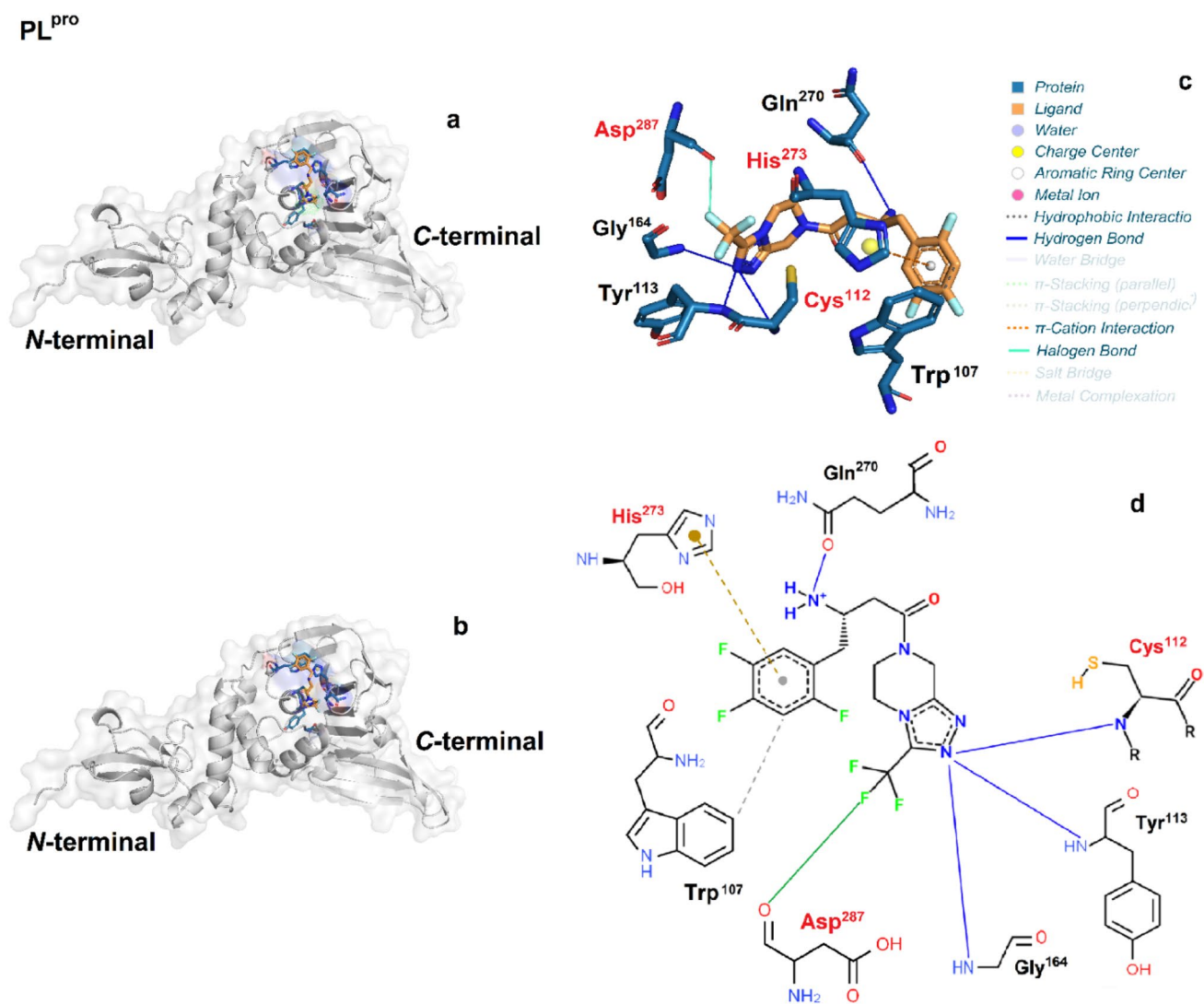
Molecular dynamics (MD) analysis demonstrated that some amino acids of the active site of PL<sup>pro</sup> and 3CL<sup>pro</sup> were capable to interact with sitagliptin, keeping a maximum distance of ligation of around 4.0 Å. After MD has been finalized, around 53.8% of PL<sup>pro</sup> amino acid residues that were kept flexible during docking simulations (Trp<sup>107</sup>, Cys<sup>112</sup>, Tyr<sup>113</sup>, Gly<sup>164</sup>, Gln<sup>270</sup>, His<sup>273</sup>, and Asp<sup>287</sup>) interacted with sitagliptin. From all the residues that were allowed to be flexible in 3CL<sup>pro</sup> (Thr<sup>26</sup>, His<sup>41</sup>, Gly<sup>143</sup>, Cys<sup>145</sup>, His<sup>163</sup>, Glu<sup>166</sup>, and Gln<sup>189</sup>), 43% showed some interaction with the ligand (Figs. 2a, b, 3a, b). The MD results show that both PL<sup>pro</sup>-sitagliptin and 3CL<sup>pro</sup>-sitagliptin complexes encompass a network characterized by the presence of charge and aromatic ring centers, hydrophobic interactions, hydrogen bonds, and  $\pi$ -cation (Figs. 2c, d, 3c, d, and Supplementary materials 1 and 2).

Figure 4 compares the root-mean-square deviation (RMSD) and the radius of gyration ( $R_g$ ) of PL<sup>pro</sup> and 3CL<sup>pro</sup> uncomplexed or complexed with the ligand. A steady RMSD of around 0.2 nm during all the simulation time (25 ns) was observed for 3CL<sup>pro</sup> (Fig. 4c), while a slight variation on the stability of the PL<sup>pro</sup>-sitagliptin complex has been observed, especially in the range of 15–25 ns (Fig. 4a). This result suggests that, as a target, PL<sup>pro</sup> appears to have less affinity to sitagliptin than 3CL<sup>pro</sup>, despite both proteins had shown similar ligation energies with  $\Delta G$  values of  $-7.8$  and  $-7.5$  kcal mol<sup>-1</sup>, for 3CL<sup>pro</sup> and PL<sup>pro</sup>, respectively. The variation on the  $R_g$  as a function of time of simulation was also a little different in both systems with the PL<sup>pro</sup>-sitagliptin complex displaying a profile that likely indicates a more compact and rigid folding of the target protein (Fig. 4b). In contrast, the 3L<sup>pro</sup>-sitagliptin complex showed a more relaxed and favorable conformation which is observed by the tendency of increase in the  $R_g$  values when compared to the non-complexed (uncomplexed) target, mainly at the final nanoseconds of the simulation (Fig. 4d). All together these results suggest that 3CL<sup>pro</sup> seemingly behaves as a better target for sitagliptin than PL<sup>pro</sup> which clearly displayed a less stable interaction.

## Discussion

Pockets and cavities in receptors usually coincide with the active sites responsible for the biological processes; therefore, it is fundamental to pay close attention to them. The precise mapping of binding hotspots for macromolecules was determined for the catalytic pockets of SARS-CoV-2 PL<sup>pro</sup> and 3CL<sup>pro</sup> proteases, after the analysis of different positions with small organic molecules as probes. Canonically, hotspots are regions on the surface of a protein with the major contributions to the ligand binding free energy. The combination of the results obtained in our work revealed the presence of three “hotspots” in PL<sup>pro</sup> (Fig. 2a) and one “hotspot” in 3CL<sup>pro</sup> (Fig. 3a) as regions that can contribute to the ligand binding free energy (Gibbs free energy).

On the other hand, in silico prediction of sitagliptin ligand, using the Molinspiration Virtual Screening, indicated a bioactivity score of 0.56, suggesting that interactions between this ligand can occur with multiple proteases. As previously reported, sitagliptin appears to be a potent inhibitor of this group of enzymes (Chittepu et al. 2019; Abbas and Hegazy 2020; Solerte et al. 2020). Furthermore, the analysis with Molinspiration also suggested that sitagliptin has the ability (0.25) to bind to G protein-coupled receptors (GPCR) and poor capacity to inhibit protein kinases (0.01). Analysis using the ChEMBL server (Mendez et al. 2019) suggested a possible activity of sitagliptin against proteases belonging to two human viruses (Table 1). A previous study reported that the use of gliptins in the treatment of type-II diabetes attenuated the risk of several kind of infections including human viral infections (Yang et al. 2016). Based on the analysis presented by the ChEMBL server the sitagliptin was predicted to be able to bind and inhibit two viral proteins: an integrase from *Immunodeficiency virus 1*, and an RNA-dependent RNA polymerase from *Hepatitis C virus NS<sub>5B</sub>*, with a confidence score value of 90%, according to a confidence level greater than 30%. Other reports have demonstrated a correlation among sitagliptin, diabetes, and HIV infection (Best et al. 2015). Taking together these results



**Fig. 2** Three putative hotspots were detected in the PL<sup>pro</sup> receptor (PDB ID: 2FE8) using the CASTp 3.0, FTSite, and FTMap servers. **a** One cavity, which is the biggest, was called S<sub>1</sub> (green color). **b**

are in agreement with our findings. In addition, the server showed that sitagliptin is also capable to bind and inhibit the human DPP<sub>4</sub>, as expected, as demonstrated by a confidence level greater than 30%.

Here, we show that the catalytic site of PL<sup>pro</sup> contains an active site formed by the classic catalytic triad (Cys<sup>112</sup>, His<sup>273</sup>, and Asp<sup>287</sup>) which are well conserved in terms of positioning and functionality at the interface of the thumb and palm sub-domains (Supplementary material 1). When the catalytic site of PL<sup>pro</sup> is not occupied by a ligand, the Cys<sup>112</sup> is positioned at the N-terminal region of an  $\alpha$ -helix  $\alpha^4$  in the thumb domain with the side chain sulfur atom being stabilized at a 3.7 Å distance from the pros( $\pi$ )-nitrogen atom of the His<sup>273</sup>. This histidine is located at the foot of the palm domain, near to the flexible loop BL<sub>2</sub>, also known

The predicted binding pocket of PL<sup>pro</sup>. **c** and **d** The 3D and 2D visualizations of the complex established by the interaction between PL<sup>pro</sup> amino acids and the sitagliptin ligand

as Gly<sup>267</sup>–Gly<sup>272</sup> loop (Ratia et al. 2006) or  $\beta$ -turn (Báez-Santos et al. 2014). In contrast, one of the oxygen atoms of the side chain of Asp<sup>287</sup> is located at a 2.7 Å distance from the *tele*( $\tau$ )-nitrogen of the His<sup>273</sup> residue at the foot of the palm domain, while the side chain of Trp<sup>107</sup> is buried inside the oxyanion hole. In addition, the indole-ring nitrogen of Trp<sup>107</sup> seems to be pivotal for the stabilization of negatively charged tetrahedral intermediates produced throughout the reaction. Remarkably, in vitro experiments using PL<sup>pro</sup> protease inhibitors showed that those inhibitors were prone to interact and bind in a cavity next to the catalytic triad (Báez-Santos et al. 2014).

Our results suggest that SARS-CoV-2 protease PL<sup>pro</sup> can be a potential receptor for the sitagliptin ligand, as verified by the binding free energy of the interaction

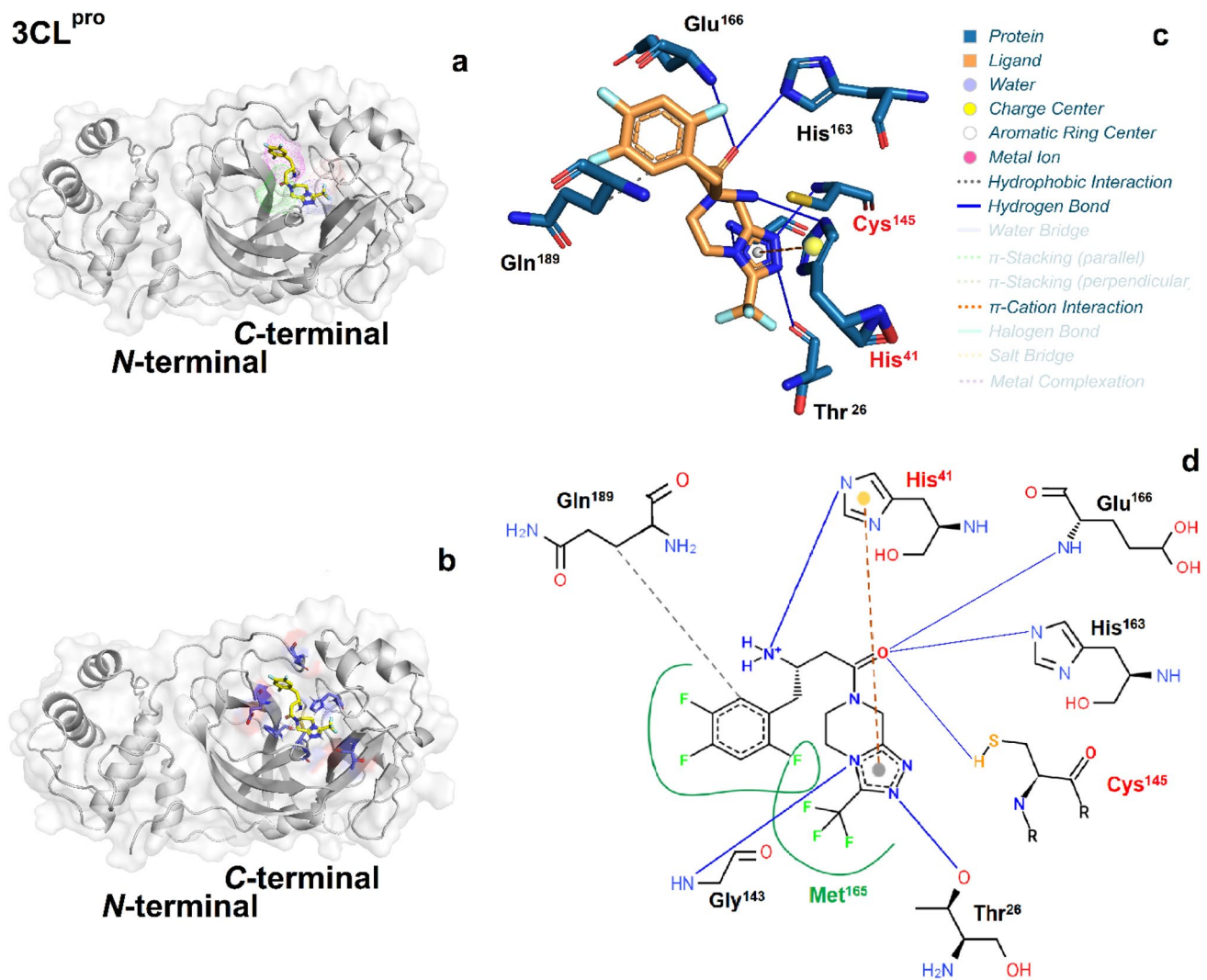


**Fig. 3** Three putative hotspots were detected in the 3CL<sup>pro</sup> receptor (PDB id: 6M2Q) using the CASTp 3.0, FTSite, and FTMap servers. **a** One cavity, which is the biggest, was called S<sub>1</sub> (magenta color), while the other three smaller cavities were called S<sub>2</sub> (green color), S<sub>3</sub>

(salmon color), and S<sub>4</sub> (slate color). **b** The predicted binding pocket of 3CL<sup>pro</sup>. **c** and **d** The 3D and 2D visualization and interaction within the amino acids of 3CL<sup>pro</sup> and ligand (sitagliptin) complex

( $\Delta G = -7.5 \text{ kcal mol}^{-1}$ ). The results point to a molecular mechanism of interaction by which sitagliptin forms a covalent adduct with PL<sup>pro</sup> protease through direct interaction with the Cys<sup>112</sup> residue with high statistic confidence. The stable binding between the nitrile group of Cys<sup>112</sup> and sitagliptin molecule would result in an inhibition of the PL<sup>pro</sup> activity (Supplementary material 2), thereby potentially inhibiting the natural pathway of SARS-CoV-2 replication. A number of compounds have been identified, using in silico approaches, as potential inhibitors of the PL<sup>pro</sup> catalytic site (Table 2), with Gibbs free energy ranging from  $-10.9$  to  $-6.5 \text{ kcal mol}^{-1}$ . Therefore, the Gibbs free energy obtained in our analysis is in agreement with previous analysis which used the PL<sup>pro</sup> protease as a ligand receptor. Different scientific approaches have demonstrated that negative

functional implications of the innate immune response during SARS-CoV-2 infection can occur due to the presence of the PL<sup>pro</sup>. In so many cases, PL<sup>pro</sup> have been implicated in functions such as deubiquitinating (DUB) and deISGylating (deISG) during cellular infection by SARS-CoV-2, removing the ubiquitin (Ub) using a chemical mechanism similar to the ubiquitin-like protein ISG<sub>15</sub>-interferon-stimulated gene 15 (Clasman et al. 2020). Therefore, increasing pools of ISG<sub>15</sub> are capable of modulation by downregulating USP<sub>18</sub> (ubiquitin-specific protease 18) levels, resulting, in turn, in the upregulation of IFN- $\alpha/\beta$  exacerbated signaling in COVID-19 patients (Mielech et al. 2014; Speer et al. 2016; Moustaqil et al. 2021).

In addition, inhibition of the synthesis of cytokines involved in the activation of the host's innate immune

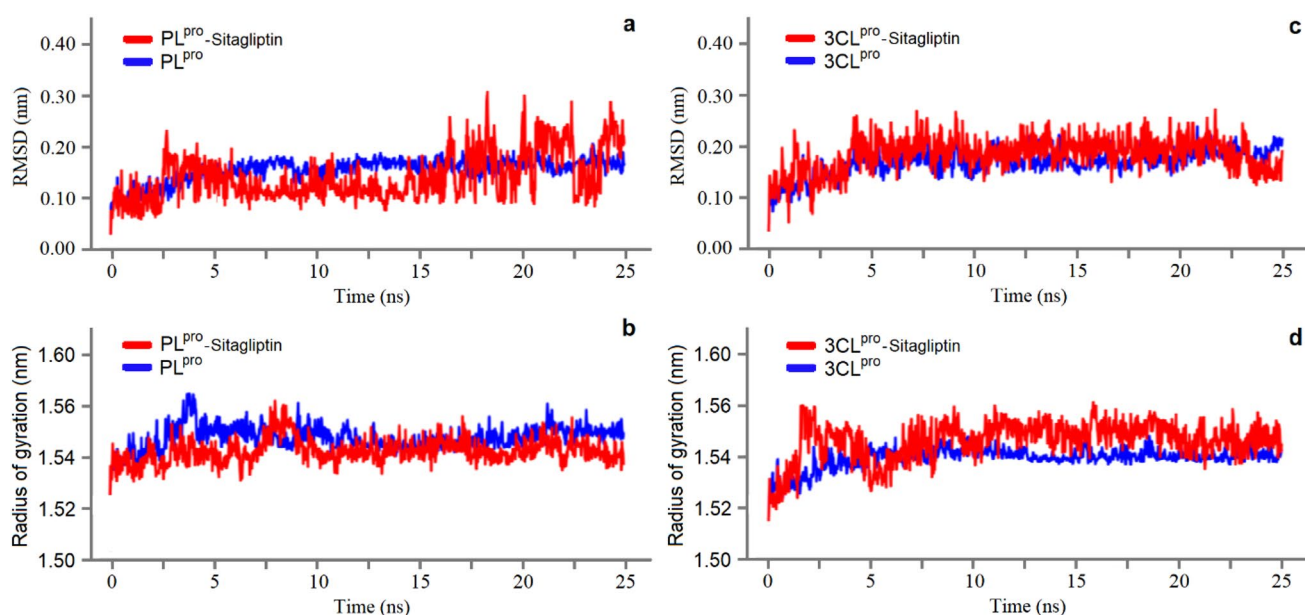


**Fig. 4** Root-mean-square deviations (RMSD) of the backbone and radius of gyration ( $R_g$ ) of the proteins from 25 ns long MD trajectory. **a** and **c** visualization of RMSD of PL<sup>pro</sup> and 3CL<sup>pro</sup> uncomplexed (blue) and complexed (red). **b** and **d** visualization of Rg of PL<sup>pro</sup> and 3CL<sup>pro</sup> uncomplexed (blue) and complexed (red)

**Table 2** In silico studies reporting molecules potentially able to inhibit SARS-CoV-2 PL<sup>pro</sup> protease

PubChem Cid	$\Delta G$ (kcal mol <sup>-1</sup> )	Interacting residues	Refs
Darunavir (24941262)	-8.7	Lys <sup>105</sup> , Trp <sup>106</sup> , Leu <sup>162</sup> , Asp <sup>164</sup> , Pro <sup>248</sup> , Tyr <sup>264</sup> , Asn <sup>267</sup> , Tyr <sup>268</sup> , Asp <sup>286</sup> , Ala <sup>288</sup>	Li et al. (2021)
Cyanidin-3-O-glucoside (165558)	-9.4	Lys <sup>157</sup> , Leu <sup>162</sup> , Asp <sup>164</sup> , Arg <sup>166</sup> , Glu <sup>167</sup> , Tyr <sup>264</sup> , Tyr <sup>268</sup> , Gln <sup>269</sup> , Gly <sup>271</sup> , Thr <sup>301</sup>	Pitsillou et al. (2020)
Hypericin (3663)	-6.5	Leu <sup>162</sup> , Gly <sup>163</sup> , Asp <sup>164</sup> , Tyr <sup>264</sup> , Tyr <sup>268</sup> , Gln <sup>269</sup> , Gly <sup>271</sup> , Tyr <sup>273</sup>	Pitsillou et al. (2020)
Rutin (5280805)	-10.9	Asp <sup>164</sup> , Arg <sup>166</sup> , Glu <sup>167</sup> , Tyr <sup>264</sup> , Tyr <sup>268</sup> , Gln <sup>269</sup> , Gly <sup>271</sup> , Thr <sup>301</sup>	Pitsillou et al. (2020)
(-)-epigallocatechin gallate (65064)	-7.9	Lys <sup>157</sup> , Gly <sup>163</sup> , Asp <sup>164</sup> , Arg <sup>166</sup> , Glu <sup>167</sup> , Tyr <sup>264</sup> , Tyr <sup>268</sup> , Gln <sup>269</sup> , Gly <sup>271</sup> , Thr <sup>301</sup>	Pitsillou et al. (2020)
Stock 1N <sub>69160</sub> (33201386)	-8.4	Gly <sup>164</sup> , Asp <sup>165</sup> , Arg <sup>167</sup> , Tyr <sup>265</sup> , Tyr <sup>269</sup> , Gln <sup>270</sup>	Elekofehinti et al. (2021)
Quercetin 374-triglucoside-44259184	-8.6	Leu <sup>211</sup> , Ser <sup>212</sup> , Tyr <sup>213</sup> , Glu <sup>214</sup> , Lys <sup>217</sup> , Tyr <sup>251</sup> , Glu <sup>252</sup> , Lys <sup>254</sup> , Gly <sup>256</sup> , Thr <sup>257</sup> , Phe <sup>258</sup> , Thr <sup>259</sup> , Ser <sup>278</sup> , Lys <sup>279</sup> , Tyr <sup>305</sup> , Lys <sup>306</sup> , Glu <sup>307</sup> , Asn <sup>308</sup> , Ser <sup>309</sup> , Tyr <sup>310</sup>	Adegbola et al. (2021)
Isorhamnetin 4-glucoside (44259381)	-8.9	Tyr <sup>213</sup> , Glu <sup>215</sup> , Lys <sup>217</sup> , Tyr <sup>251</sup> , Glu <sup>252</sup> , Leu <sup>253</sup> , Lys <sup>254</sup> , Thr <sup>257</sup> , Phe <sup>258</sup> , Tyr <sup>305</sup> , Lys <sup>306</sup> , Glu <sup>307</sup> , Tyr <sup>310</sup>	Adegbola et al. (2021)

response against the SARS-CoV-2, and chemokines such as CCL<sub>5</sub> and CXCL<sub>10</sub>, seems to be associated with the presence of PL<sup>pro</sup> (Báez-Santos et al. 2015). On the other hand, the increase in C-reactive protein (CRP) and inflammatory factors in the plasma, like the interleukins IL<sub>2</sub>, IL<sub>4</sub>, IL<sub>6</sub>, IL<sub>7</sub>, IL<sub>10</sub>, IL<sub>12</sub>, IL<sub>13</sub>, IL<sub>17</sub>, TNF- $\alpha$ , GCSF, MCSF, IP<sub>10</sub>, MCP<sub>1</sub>, MIP<sub>1 $\alpha$</sub> , and HGF can trigger a cytokine storm in the body of critical patients affected by SARS-CoV-2 (Guo et al. 2020; Prompetchara et al. 2020; Singhal, 2020; Zu et al. 2020). Therefore, the discovery of new therapeutics and/or drug repositioning approaches intended to inhibit the PL<sup>pro</sup>

protease (SARS-CoV-2) are of great interest to prevent the emergence of new cases of COVID-19, since the number of cases grows up all over the world.

In addition to PL<sup>pro</sup>, SARS-CoV-2 3CL<sup>pro</sup> protease may also trigger some negative effects to the organism of infected patients such as the antagonization of IFN-stimulated response elements - ISRE (Wu et al. 2020; McGill et al. 2021; Moustaqil et al. 2021), cleavage of both the NF-kappa  $\beta$  essential modulator (NEMO), and the signal transducer and activator of transcription 2 - STAT<sub>2</sub> (Fehr et al. 2016; Chen et al. 2019) resulting in the downregulation of



IGSs, and the interaction with E<sub>3</sub> ligase of tripartite motif-containing protein 25 - TRIM<sub>25</sub> (Wu et al. 2020), and the interferon regulatory factor 3 - IRF<sub>3</sub> (Moustaqil et al. 2021). Intriguingly, 3CL<sup>PRO</sup> was also able to induce changes in the metabolism of the phosphorylation of IFN-mediated STAT<sub>1</sub>, resulting in metabolic damage due to a localized increase in the levels of autophagosomal membrane proteins - LC<sub>3</sub>B (Xia et al. 2020).

Furthermore, it was previously documented that 3CL<sup>PRO</sup> is capable of inducing the cleavage of NLR family pyrin domain containing 12 (NLRP<sub>12</sub>) and TGF-β activated kinase 1 (MAP<sub>3</sub>K<sub>7</sub>) binding protein 1 (TAB<sub>1</sub>), as well as to induce an intense synthesis of cytokines and accentuated inflammatory response in SARS-CoV-2-infected patients (Moustaqil et al. 2021).

Analysis of the 3CL<sup>PRO</sup> catalytic site showed a general topology quasi-ellipsoid due to the presence of three distinct domains (named domain I, domain II, and domain III), which are connected with flexible loops, being domains I and II related to the catalytic activity, and domain III to dimerization (Shi et al. 2004; Wang et al. 2020). The catalytic dyad His-Cys (His<sup>41</sup> and Cys<sup>145</sup>) of 3CL<sup>PRO</sup>, as previously reported in the literature (Yang et al. 2003; Das et al. 2020; Tahir ul Qamar et al. 2020), is located in a relatively shallow cavity between domains I and II defining the catalytic site (Supplementary material 3), to an optimum distance (at 3.6 Å) for hydrogen bonding interactions.

When the catalytic site of 3CL<sup>PRO</sup> is not occupied by a ligand, the side chain sulfur atom of the Cys<sup>145</sup> residue (Domain II) is located at a 3.6 Å distance from the tele(τ)-nitrogen atom of the His<sup>41</sup> residue of the α-helix 2 (α<sub>2</sub>) of the sheet A (Domain I). Alternatively, the Glu<sup>166</sup> residue also located in the Domain II is positioned at a distance in

which the presence of two water molecules is necessary for the interaction with potential inhibitors of the 3CL<sup>PRO</sup> (Table 3) catalytic site.

The binding free energy we encountered in our study suggests that SARS-CoV-2 3CL<sup>PRO</sup> protease can be a potential receptor for sitagliptin (Supplementary material 4), with a  $\Delta G = -7.8 \text{ kcal.mol}^{-1}$ . This result was nearly identical to what we found for PL<sup>PRO</sup> protease ( $\Delta G = -7.5 \text{ kcal mol}^{-1}$ ). A list of compounds (Tables 2 and 3) has been identified, using in silico approaches, as potential good inhibitors for 3CL<sup>PRO</sup> with Gibbs free energy values ranging from  $-10.9$  to  $-6.5 \text{ (kcal mol}^{-1})$ . The results obtained here agree with these observations suggesting that, as observed for PL<sup>PRO</sup>, sitagliptin may potentially be repositioned to be used as a drug directed to inhibit SARS-CoV-2 3CL<sup>PRO</sup> and consequently suppress the spread and evolution of SARS-CoV-2 infection.

Structural analyses of the dipeptidyl peptidase 4 (DPP<sub>4</sub>) showed that this molecule is a cell membrane-bound receptor, expressed at high levels. DPP<sub>4</sub> is formed by two subunits, each of one is composed by an 8-bladed β-propeller domain (N-terminal region) and an α/β hydrolase domain (C-terminal region). All known gliptins bind to a large pocket in the cavity located at the interface of the α/β-hydrolase domain and the 8-bladed β-propeller domain. The biological functions of DPP<sub>4</sub> are associated with a variety of substrates, including incretin hormones, cytokines, chemokines, neuropeptides, and growth factors (Nar et al. 2021). In the context of the infections caused by *Coronavirus*, new evidences have shown that the human DPP<sub>4</sub> is a functional receptor to SARS-CoV-2, due to the ability of the homotrimer structure of the spike protein (S<sub>1</sub> domain) to interact and bind to these receptors (Vankadari and Wilce 2020).

**Table 3** In silico studies reporting molecules potentially able to inhibit SARS-CoV-2 3CL<sup>PRO</sup> protease

PubChem Cid	$\Delta G \text{ (kcal mol}^{-1})$	Interacting residues	Refs
Baicalin (64982)	-8.1	Leu <sup>141</sup> , Asn <sup>142</sup> , Gly <sup>143</sup> , Met <sup>165</sup> , Glu <sup>166</sup> , Pro <sup>168</sup> , Gln <sup>189</sup>	Islam et al. (2020)
Carnosol (442009)	-8.2	Thr <sup>25</sup> , Thr <sup>26</sup> , Leu <sup>27</sup> , His <sup>41</sup> , Cys <sup>44</sup> , Thr <sup>45</sup> , Ser <sup>46</sup> , Met <sup>49</sup> , Asn <sup>142</sup> , Gly <sup>143</sup> , Cys <sup>145</sup> , His <sup>164</sup> , Met <sup>165</sup> , Glu <sup>166</sup> , Arg <sup>188</sup> , Gln <sup>189</sup>	Umesh et al. (2020)
Crocin (5281233)	-8.2	Phe <sup>3</sup> , Arg <sup>4</sup> , Lys <sup>5</sup> , Arg <sup>131</sup> , Asn <sup>133</sup> , Thr <sup>135</sup> , Lys <sup>137</sup> , Asp <sup>197</sup> , Thr <sup>199</sup>	Aanouz et al. (2021)
Cyanidin 3-glucoside (197081)	-8.4	Thr <sup>26</sup> , Met <sup>49</sup> , Asn <sup>142</sup> , Gly <sup>143</sup> , Cys <sup>145</sup> , His <sup>163</sup> , His <sup>164</sup> , Glu <sup>166</sup> , Asp <sup>187</sup> , Gln <sup>189</sup>	Islam et al. (2020)
Fluvastatin (446155)	-7.7	His <sup>163</sup> , Glu <sup>166</sup>	Reiner et al. (2020)
Glabridin (124052)	-8.1	His <sup>41</sup> , Met <sup>49</sup> , Leu <sup>141</sup> , Met <sup>165</sup> , Glu <sup>166</sup> ,	Islam et al. (2020)
Quercetin 3-vicianoside (44259139)	-8.3	Thr <sup>25</sup> , Thr <sup>26</sup> , His <sup>41</sup> , Leu <sup>114</sup> , Phe <sup>140</sup> , Asn <sup>142</sup> , Gly <sup>143</sup> , Ser <sup>144</sup> , Cys <sup>145</sup> , His <sup>163</sup> , His <sup>164</sup> , Met <sup>165</sup> , Glu <sup>166</sup> , Asp <sup>187</sup> , Arg <sup>188</sup> , Gln <sup>189</sup>	Bhardwaj et al. (2021)
Myricitrin (5281673)	-8.9	Thr <sup>26</sup> , Leu <sup>37</sup> , His <sup>41</sup> , Met <sup>49</sup> , Tyr <sup>54</sup> , Phe <sup>140</sup> , Leu <sup>141</sup> , Asn <sup>142</sup> , Gly <sup>143</sup> , Ser <sup>144</sup> , Cys <sup>145</sup> , His <sup>163</sup> , His <sup>164</sup> , Met <sup>165</sup> , Glu <sup>166</sup> , His <sup>172</sup> , Asp <sup>187</sup> , Arg <sup>188</sup>	Joshi et al. (2020)
Rosmanol (13966122)	-7.9	Thr <sup>25</sup> , His <sup>41</sup> , Met <sup>49</sup> , Phe <sup>140</sup> , Leu <sup>141</sup> , Asn <sup>142</sup> , Gly <sup>143</sup> , Ser <sup>144</sup> , Cys <sup>145</sup> , His <sup>163</sup> , Met <sup>165</sup> , Glu <sup>166</sup>	Umesh et al. (2020)
22-Hydroxyhopan-3-one (21582894)	-8.6	Met <sup>49</sup> , Cys <sup>145</sup> , Met <sup>165</sup> , Arg <sup>189</sup>	Gyebi et al. (2020)

Some recent studies have proposed that DPP<sub>4</sub> inhibitors (iDDP<sub>4</sub>) with antiviral action might be useful for controlling the infection caused by SARS-CoV-2, especially for patients with diabetes (Drucker 2020; Eleftheriou et al. 2020; Iacobellis 2020), a group that deserves special attention due to its elevated risk to developing the severe acute respiratory syndrome, a very serious complication of COVID-19 disease. In the context of iDDP<sub>4</sub>, a series of indirect findings suggests that these drugs could be useful therapeutic off-target effects (Valencia et al. 2020), although there are several ongoing clinical discussions. About the gliptins (iDPP<sub>4</sub> canonical class), it is important to emphasize that the use of these drugs is preferred in the treatment of individuals with diabetes, associated with chronic kidney disease or cardiovascular disease (Hansen and Jandeleit-Dahm 2019). Therapeutic applications of sitagliptin in type 2 diabetic patients reduced the levels of C-reactive protein, interleukin-6 in mononuclear cells (Hussain et al. 2019; Katsiki and Ferrannini 2020), circulating TNF- $\alpha$ , interleukin-1 $\beta$ , and intracellular adhesion molecules (Tremblay et al. 2014), while it induced an increase in flow-mediated vasodilation in diabetic adults (Barchetta et al. 2019), and cardioprotection in diabetic patients with chronic kidney disease reducing the angiotensin II/angiotensin-(1–7) ratio (Tremblay et al. 2014; Beraldo et al. 2019; Barchetta et al. 2019).

## Conclusion

By a series of in silico assays we demonstrated here that sitagliptin, a drug commonly used for treatment of type-II diabetes, exhibited potential dual-target inhibitory activity compatible with the active sites of two main SARS-CoV-2 proteases, 3CL<sup>PRO</sup>, and PL<sup>PRO</sup>. These findings justify the implementation of additional in vitro and in vivo studies aiming to validate the use of this drug as a repositioning medication in the fight against COVID-19 disease.

**Supplementary Information** The online version contains supplementary material available at <https://doi.org/10.1007/s13205-022-03406-w>.

**Author contributions** JEdCF, JEMJ, DPP, GEdCPL, CLdA, VRV, MPM, EBLF, RGO helped in conceptualization, methodology, data curation, writing—original draft preparation, validation, writing—reviewing and editing. VOF, APDRM, RCM performed visualization, investigation. RMMJ supervised the study.

## Declarations

**Conflict of interest** Authors declare that they have no conflict of interest.

**Ethical approval** This article does not contain any studies with human participants or animals.

## References

- Aanouz I, Belhassan A, El-Khatibi K et al (2021) Moroccan medicinal plants as inhibitors against SARS-CoV-2 main protease: computational investigations. *J Biomol Struct Dyn* 39:2971–2979. <https://doi.org/10.1080/07391102.2020.1758790>
- Abbas HA, Hegazy WAH (2020) Repurposing anti-diabetic drug “Sitagliptin” as a novel virulence attenuating agent in *Serratia marcescens*. *PLoS ONE* 15:e0231625. <https://doi.org/10.1371/journal.pone.0231625>
- Abd-Elsalam S, Noor RA, Badawi R et al (2021) Clinical study evaluating the efficacy of ivermectin in COVID-19 treatment: a randomized controlled study. *J Med Virol* 93:5833–5838. <https://doi.org/10.1002/jmv.27122>
- Abdizadeh R, Hadizadeh F, Abdizadeh T (2022) *In silico* analysis and identification of antiviral coumarin derivatives against 3-chymotrypsin-like main protease of the novel coronavirus SARS-CoV-2. *Mol Divers* 26:1053–1076. <https://doi.org/10.1007/s11030-021-10230-6>
- Abraham MJ, Murtola T, Schulz R et al (2015) GROMACS: High performance molecular simulations through multi-level parallelism from laptops to supercomputers. *SoftwareX* 1–2:19–25. <https://doi.org/10.1016/j.softx.2015.06.001>
- Adasme MF, Linnemann KL, Bolz SN et al (2021) PLIP 2021: expanding the scope of the protein–ligand interaction profiler to DNA and RNA. *Nucleic Acids Res* 49:W530–W534. <https://doi.org/10.1093/nar/gkab294>
- Adegbola PI, Semire B, Fadahunsi OS, Adegoke AE (2021) Molecular docking and ADMET studies of *Allium cepa*, *Azadirachta indica* and *Xylopiya aethiopica* isolates as potential anti-viral drugs for Covid-19. *Virus Dis* 32:85–97. <https://doi.org/10.1007/s13337-021-00682-7>
- Amaral CML, Magalhaes ICL, Bezerra AS et al (2022) Insight into possible adjuvant role of phytol to fight SARS-CoV-2. *Curr Sci* 122:1241–1242
- Báez-Santos YM, Barraza SJ, Wilson MW et al (2014) X-ray structural and biological evaluation of a series of potent and highly selective inhibitors of human coronavirus papain-like proteases. *J Med Chem* 57:2393–2412. <https://doi.org/10.1021/jm401712t>
- Báez-Santos YM, St. John SE, Mesecar AD (2015) The SARS-coronavirus papain-like protease: structure, function and inhibition by designed antiviral compounds. *Antiviral Res* 115:21–38. <https://doi.org/10.1016/j.antiviral.2014.12.015>
- Barchetta I, Ciccarelli G, Barone E et al (2019) Greater circulating DPP<sub>4</sub> activity is associated with impaired flow-mediated dilatation in adults with type 2 diabetes mellitus. *Nutr Metab Cardiovasc Dis* 29:1087–1094. <https://doi.org/10.1016/j.numecd.2019.07.010>
- Beraldo JI, Benetti A, Borges-Júnior FA et al (2019) Cardioprotection conferred by sitagliptin is associated with reduced cardiac angiotensin II/angiotensin-(1–7) balance in experimental chronic kidney disease. *Int J Mol Sci* 20:1940. <https://doi.org/10.3390/ijms20081940>
- Berendsen HJC, Postma JPM, Van Gunsteren WF et al (1984) Molecular dynamics with coupling to an external bath. *J Chem Phys* 81:3684–3690. <https://doi.org/10.1063/1.448118>
- Best C, Struthers H, Laciny E et al (2015) Sitagliptin reduces inflammation and chronic immune cell activation in HIV<sup>+</sup> adults with impaired glucose tolerance. *J Clin Endocrinol Metab* 100:2621–2629. <https://doi.org/10.1210/jc.2015-1531>
- Bhardwaj VK, Singh R, Sharma J et al (2021) Identification of bioactive molecules from tea plant as SARS-CoV-2 main protease inhibitors. *J Biomol Struct Dyn* 39:3449–3458. <https://doi.org/10.1080/07391102.2020.1766572>

- Blum M, Chang H-Y, Chuguransky S et al (2021) The InterPro protein families and domains database: 20 years on. *Nucleic Acids Res* 49:D344–D354. <https://doi.org/10.1093/nar/gkaa977>
- Burley SK, Bhikadiya C, Bi C et al (2021) RCSB Protein Data Bank: powerful new tools for exploring 3D structures of biological macromolecules for basic and applied research and education in fundamental biology, biomedicine, biotechnology, bioengineering and energy sciences. *Nucleic Acids Res* 49:D437–D451. <https://doi.org/10.1093/nar/gkaa1038>
- Chen S, Tian J, Li Z et al (2019) Feline infectious peritonitis virus NSP<sub>5</sub> inhibits type I interferon production by cleaving NEMO at multiple sites. *Viruses* 12:43. <https://doi.org/10.3390/v12010043>
- Chittepu VCSR, Kalhotra P, Osorio-Gallardo T et al (2019) New molecular insights into the inhibition of dipeptidyl peptidase-4 by natural cyclic peptide oxytocin. *Molecules* 24:3887. <https://doi.org/10.3390/molecules24213887>
- Clasman JR, Everett RK, Srinivasan K, Mesecar AD (2020) Decoupling deISGylating and deubiquitinating activities of the MERS virus papain-like protease. *Antiviral Res* 174:104661. <https://doi.org/10.1016/j.antiviral.2019.104661>
- Cui J, Li F, Shi Z-L (2019) Origin and evolution of pathogenic coronaviruses. *Nat Rev Microbiol* 17:181–192. <https://doi.org/10.1038/s41579-018-0118-9>
- Das S, Sarmah S, Lyndem S, Singha Roy A (2020) An investigation into the identification of potential inhibitors of SARS-CoV-2 main protease using molecular docking study. *J Biomol Struct Dyn*. <https://doi.org/10.1080/07391102.2020.1763201>
- Denison MR, Graham RL, Donaldson EF et al (2011) Coronaviruses—an RNA proofreading machine regulates replication fidelity and diversity. *RNA Biol* 8:270–279. <https://doi.org/10.4161/rna.8.2.15013>
- Drucker DJ (2020) Coronavirus infections and type 2 diabetes—shared pathways with therapeutic implications. *Endocr Rev* 41:457–470. <https://doi.org/10.1210/edrv/bnaa011>
- Eleftheriou P, Amanatidou D, Petrou A, Geronikaki A (2020) *In silico* evaluation of the effectivity of approved protease inhibitors against the main protease of the novel SARS-CoV-2 virus. *Molecules* 25:2529. <https://doi.org/10.3390/molecules25112529>
- Elekofehinti OO, Iwaloye O, Josiah SS et al (2021) Molecular docking studies, molecular dynamics and ADME/tox reveal therapeutic potentials of STOCK1N-69160 against papain-like protease of SARS-CoV-2. *Mol Divers* 25:1761–1773. <https://doi.org/10.1007/s11030-020-10151-w>
- Essmann U, Perera L, Berkowitz ML et al (1995) A smooth particle mesh Ewald method. *J Chem Phys* 103:8577–8593. <https://doi.org/10.1063/1.470117>
- Fan C, Wu X, Liu Q et al (2018) A human DPP<sub>4</sub>-knockin mouse's susceptibility to infection by authentic and pseudotyped MERS-CoV. *Viruses* 10:448. <https://doi.org/10.3390/v10090448>
- Fehr AR, Channappanavar R, Jankevicius G et al (2016) The conserved *Coronavirus* macrodomain promotes virulence and suppresses the innate immune response during severe acute respiratory syndrome Coronavirus infection. *Mbio* 7:1–12. <https://doi.org/10.1128/mBio.01721-16>
- Freire CMAS, Fonseca FMP, Evangelista AJJ et al (2020) SARS-CoV2: a brief analysis of the history of an asymptomatic patient. *Sylvan* 164:486–505
- Green JB, Bethel MA, Armstrong PW et al (2015) Effect of sitagliptin on cardiovascular outcomes in type 2 diabetes. *N Engl J Med* 373:232–242. <https://doi.org/10.1056/NEJMoa1501352>
- Guo Y, Cao Q, Hong Z et al (2020) The origin, transmission and clinical therapies on coronavirus disease 2019 (COVID-19) outbreak—an update on the status. *Mil Med Res* 7:11. <https://doi.org/10.1186/s40779-020-00240-0>
- Gyebi GA, Ogunro OB, Adegunloye AP et al (2020) Potential inhibitors of coronavirus 3-chymotrypsin-like protease (3CL pro): an *in silico* screening of alkaloids and terpenoids from African medicinal plants. *J Biomol Struct Dyn*. <https://doi.org/10.1080/07391102.2020.1764868>
- Hanssen NM, Jandeleit-Dahm KA (2019) Dipeptidyl peptidase-4 inhibitors and cardiovascular and renal disease in type 2 diabetes: what have we learned from the CARMELINA trial? *Diabetes Vasc Dis Res* 16:303–309. <https://doi.org/10.1177/1479164119842339>
- Hess B (2008) P-LINCS: a parallel linear constraint solver for molecular simulation. *J Chem Theory Comput* 4:116–122. <https://doi.org/10.1021/ct700200b>
- Huang Y, Yang C, Xu X et al (2020) Structural and functional properties of SARS-CoV-2 spike protein: potential antiviral drug development for COVID-19. *Acta Pharmacol Sin* 41:1141–1149. <https://doi.org/10.1038/s41401-020-0485-4>
- Hussain M, Rafique MA, Iqbal J, Akhtar L (2019) Effect of sitagliptin and glimepiride on C-reactive protein (CRP) in overweight Type-2 diabetic patients. *Pakistan J Med Sci* 35:1–5. <https://doi.org/10.12669/pjms.35.2.645>
- Iacobellis G (2020) COVID-19 and diabetes: can DPP<sub>4</sub> inhibition play a role? *Diabetes Res Clin Pract* 162:108125. <https://doi.org/10.1016/j.diabres.2020.108125>
- Islam R, Parves MR, Paul AS et al (2020) A molecular modeling approach to identify effective antiviral phytochemicals against the main protease of SARS-CoV-2. *J Biomol Struct Dyn* 2020:1–12. <https://doi.org/10.1080/07391102.2020.1761883>
- Joshi RS, Jagdale SS, Bansode SB et al (2020) Discovery of potential multi-target-directed ligands by targeting host-specific SARS-CoV-2 structurally conserved main protease. *J Biomol Struct Dyn*. <https://doi.org/10.1080/07391102.2020.1760137>
- Kashour Z, Riaz M, Garbati MA et al (2021) Efficacy of chloroquine or hydroxychloroquine in COVID-19 patients: a systematic review and meta-analysis. *J Antimicrob Chemother* 76:30–42. <https://doi.org/10.1093/jac/dkaa403>
- Katsiki N, Ferrannini E (2020) Anti-inflammatory properties of anti-diabetic drugs: a “promised land” in the COVID-19 era? *J Diabetes Complications* 34:107723. <https://doi.org/10.1016/j.jdiacomp.2020.107723>
- Kozakov D, Grove LE, Hall DR et al (2015) The FTMap family of web servers for determining and characterizing ligand-binding hot spots of proteins. *Nat Protoc* 10:733–755. <https://doi.org/10.1038/nprot.2015.043>
- Li K, Wohlford-Lenane CL, Channappanavar R et al (2017) Mouse-adapted MERS coronavirus causes lethal lung disease in human DPP<sub>4</sub> knockin mice. *Proc Natl Acad Sci* 114:E3119–E3128. <https://doi.org/10.1073/pnas.1619109114>
- Li Y, Zhang Z, Yang L et al (2020) The MERS-CoV receptor DPP<sub>4</sub> as a candidate binding target of the SARS-CoV-2 spike. *iScience* 23:101160. <https://doi.org/10.1016/j.isci.2020.101160>
- Li D, Luan J, Zhang L (2021) Molecular docking of potential SARS-CoV-2 papain-like protease inhibitors. *Biochem Biophys Res Commun* 538:72–79. <https://doi.org/10.1016/j.bbrc.2020.11.083>
- Lu S, Wang J, Chitsaz F et al (2020) CDD/SPARCLE: the conserved domain database in 2020. *Nucleic Acids Res* 48:D265–D268. <https://doi.org/10.1093/nar/gkz991>
- McGill AR, Kahlil R, Dutta R et al (2021) SARS-CoV-2 Immunopathogenesis and potential for diverse vaccines and therapies: opportunities and challenges. *Infect Dis Rep* 13:102–125. <https://doi.org/10.3390/idr13010013>
- Mendez D, Gaulton A, Bento AP et al (2019) ChEMBL: towards direct deposition of bioassay data. *Nucleic Acids Res* 47:D930–D940. <https://doi.org/10.1093/nar/gky1075>
- Mielech AM, Chen Y, Mesecar AD, Baker SC (2014) *Nidovirus* papain-like proteases: multifunctional enzymes with protease, deubiquitinating and deISGylating activities. *Virus Res* 194:184–190. <https://doi.org/10.1016/j.virusres.2014.01.025>



- Moustaqil M, Ollivier E, Chiu H-P et al (2021) SARS-CoV-2 proteases PL<sup>pro</sup> and 3CL<sup>pro</sup> cleave IRF3 and critical modulators of inflammatory pathways (NLRP12 and TAB1): implications for disease presentation across species. *Emerg Microbes Infect* 10:178–195. <https://doi.org/10.1080/22221751.2020.1870414>
- Nar H, Schnapp G, Hucke O et al (2021) Action of dipeptidyl peptidase-4 inhibitors on SARS-CoV-2 main protease. *ChemMedChem* 16:1425–1426. <https://doi.org/10.1002/cmdc.202000921>
- Narayanan A, Narwal M, Majowicz SA et al (2022) Identification of SARS-CoV-2 inhibitors targeting Mpro and PLpro using in-cell-protease assay. *Commun Biol* 5:169. <https://doi.org/10.1038/s42003-022-03090-9>
- Ngan C, Hall DR, Zerbe B et al (2012) FTSite: high accuracy detection of ligand binding sites on unbound protein structures. *Bioinformatics* 28:286–287. <https://doi.org/10.1093/bioinformatics/btr651>
- Pitsillou E, Liang J, Ververis K et al (2020) Identification of small molecule inhibitors of the deubiquitinating activity of the SARS-CoV-2 papain-like protease: *in silico* molecular docking studies and *in vitro* enzymatic activity assay. *Front Chem* 8:1–15. <https://doi.org/10.3389/fchem.2020.623971>
- Prompetchara E, Ketloy C, Palaga T (2020) Immune responses in COVID-19 and potential vaccines: lessons learned from SARS and MERS epidemic. *Asian Pacific J Allergy Immunol* 38:1–9. <https://doi.org/10.12932/AP-200220-0772>
- Ratia K, Saikatendu KS, Santarsiero BD et al (2006) Severe acute respiratory syndrome coronavirus papain-like protease: structure of a viral deubiquitinating enzyme. *Proc Natl Acad Sci* 103:5717–5722. <https://doi.org/10.1073/pnas.0510851103>
- Ravi V, Saxena S, Panda PS (2022) Basic virology of SARS-CoV 2. *Indian J Med Microbiol* 40:182–186. <https://doi.org/10.1016/j.ijmb.2022.02.005>
- Reiner Ž, Hatamipour M, Banach M et al (2020) Statins and the COVID-19 main protease: *in silico* evidence on direct interaction. *Arch Med Sci* 16:490–496. <https://doi.org/10.5114/aoms.2020.94655>
- Scheen AJ (2013) Cardiovascular effects of gliptins. *Nat Rev Cardiol* 10:73–84. <https://doi.org/10.1038/nrcardio.2012.183>
- Schöning-Stierand K, Diedrich K, Fährrolfes R et al (2020) Protein-sPlus: interactive analysis of protein–ligand binding interfaces. *Nucleic Acids Res* 48:W48–W53. <https://doi.org/10.1093/nar/gkaa235>
- Shi J, Wei Z, Song J (2004) Dissection study on the severe acute respiratory syndrome 3C-like protease reveals the critical role of the extra domain in dimerization of the enzyme. *J Biol Chem* 279:24765–24773. <https://doi.org/10.1074/jbc.M311744200>
- Sigrist CJA, de Castro E, Cerutti L et al (2012) New and continuing developments at PROSITE. *Nucleic Acids Res* 41:D344–D347. <https://doi.org/10.1093/nar/gks1067>
- Singh R, Bhardwaj VK, Sharma J et al (2021) Identification of potential plant bioactive as SARS-CoV-2 Spike protein and human ACE<sub>2</sub> fusion inhibitors. *Comput Biol Med* 136:104631. <https://doi.org/10.1016/j.combiomed.2021.104631>
- Singh R, Bhardwaj VK, Das P et al (2022) Benchmarking the ability of novel compounds to inhibit SARS-CoV-2 main protease using steered molecular dynamics simulations. *Comput Biol Med* 146:105572. <https://doi.org/10.1016/j.combiomed.2022.105572>
- Singhal T (2020) A review of *Coronavirus* disease-2019 (COVID-19). *Indian J Pediatr* 87:281–286. <https://doi.org/10.1007/s12098-020-03263-6>
- Solerte SB, Di Sabatino A, Galli M, Fiorina P (2020) Dipeptidyl peptidase-4 (DPP<sub>4</sub>) inhibition in COVID-19. *Acta Diabetol* 57:779–783. <https://doi.org/10.1007/s00592-020-01539-z>
- Speer SD, Li Z, Buta S et al (2016) ISG15 deficiency and increased viral resistance in humans but not mice. *Nat Commun* 7:11496. <https://doi.org/10.1038/ncomms11496>
- Su H, Yao S, Zhao W et al (2020) Anti-SARS-CoV-2 activities *in vitro* of Shuanghuanglian preparations and bioactive ingredients. *Acta Pharmacol Sin* 41:1167–1177. <https://doi.org/10.1038/s41401-020-0483-6>
- Tahir ul Qamar M, Alqahtani SM, Alamri MA, Chen L (2020) Structural basis of SARS-CoV-2 3CL<sup>pro</sup> and anti-COVID-19 drug discovery from medicinal plants. *J Pharm Anal* 10:313–319. <https://doi.org/10.1016/j.jpha.2020.03.009>
- Tian W, Chen C, Lei X et al (2018) CASTp 3.0: computed atlas of surface topography of proteins. *Nucleic Acids Res* 46:W363–W367. <https://doi.org/10.1093/nar/gky473>
- Tremblay AJ, Lamarche B, Deacon CF et al (2014) Effects of sitagliptin therapy on markers of low-grade inflammation and cell adhesion molecules in patients with type 2 diabetes. *Metabolism* 63:1141–1148. <https://doi.org/10.1016/j.metabol.2014.06.004>
- Trott L, Olson AJ (2010) AutoDock Vina: improving the speed and accuracy of docking with a new scoring function, efficient optimization and multithreading. *J Comput Chem* 31:455–461. <https://doi.org/10.1002/jcc.21334>
- Umesh KD, Selvaraj C et al (2020) Identification of new anti-nCoV drug chemical compounds from Indian spices exploiting SARS-CoV-2 main protease as target. *J Biomol Struct Dyn*. <https://doi.org/10.1080/07391102.2020.1763202>
- Valencia I, Peiró C, Lorenzo Ó et al (2020) DPP<sub>4</sub> and ACE<sub>2</sub> in diabetes and COVID-19: therapeutic targets for cardiovascular complications? *Front Pharmacol* 11:1–14. <https://doi.org/10.3389/fphar.2020.01161>
- Vankadari N, Wilce JA (2020) Emerging COVID-19 coronavirus: glycan shield and structure prediction of spike glycoprotein and its interaction with human CD26. *Emerg Microbes Infect* 9:601–604. <https://doi.org/10.1080/22221751.2020.1739565>
- Wang H, He S, Deng W et al (2020) Comprehensive insights into the catalytic mechanism of middle east respiratory syndrome 3C-like protease and severe acute respiratory syndrome 3C-like protease. *ACS Catal* 10:5871–5890. <https://doi.org/10.1021/acscatal.0c00110>
- Wu Y, Ma L, Zhuang Z et al (2020) Main protease of SARS-CoV-2 serves as a bifunctional molecule in restricting type I interferon antiviral signaling. *Signal Transduct Target Ther* 5:221. <https://doi.org/10.1038/s41392-020-00332-2>
- Xia H, Cao Z, Xie X et al (2020) Evasion of type I interferon by SARS-CoV-2. *Cell Rep* 33:108234. <https://doi.org/10.1016/j.celrep.2020.108234>
- Yang H, Yang M, Ding Y et al (2003) The crystal structures of severe acute respiratory syndrome virus main protease and its complex with an inhibitor. *Proc Natl Acad Sci* 100:13190–13195. <https://doi.org/10.1073/pnas.1835675100>
- Yang W, Cai X, Han X, Ji L (2016) DPP-4 inhibitors and risk of infections: a meta-analysis of randomized controlled trials. *Diabetes Metab Res Rev* 32:391–404. <https://doi.org/10.1002/dmrr.2723>
- Yavarian J, Nejati A, Salimi V et al (2022) Whole genome sequencing of SARS-CoV2 strains circulating in Iran during five waves of pandemic. *PLoS ONE* 17:e0267847. <https://doi.org/10.1371/journal.pone.0267847>
- Yilmaz E, Akyön Y, Serdar M (2020) The molecular footprints of COVID-19. *Turkish J Biochem* 45:241–248. <https://doi.org/10.1515/tjb-2020-0255>
- Yoshikawa K, Tsuchiya A, Kido T et al (2020) Long-term safety and efficacy of sitagliptin for type 2 diabetes mellitus in Japan: results of a multicentre, open-label, observational post-marketing surveillance study. *Adv Ther* 37:2442–2459. <https://doi.org/10.1007/s12325-020-01293-2>
- Zhao Y, Tian Y, Pan C et al (2022) Target-based *in silico* screening for phytoactive compounds targeting SARS-CoV-2. *Interdiscip Sci Comput Life Sci* 14:64–79. <https://doi.org/10.1007/s12539-021-00461-4>

















Zu ZY, Di JM, Xu PP et al (2020) *Coronavirus* disease 2019 (COVID-19): a perspective from China. *Radiology* 296:E15–E25. <https://doi.org/10.1148/radiol.2020200490>

Springer Nature or its licensor (e.g. a society or other partner) holds

exclusive rights to this article under a publishing agreement with the author(s) or other rightsholder(s); author self-archiving of the accepted manuscript version of this article is solely governed by the terms of such publishing agreement and applicable law.

## Authors and Affiliations

José Ednézio da Cruz Freire<sup>1,2,3</sup>  · José Edvar Monteiro Júnior<sup>4</sup>  · Daniel Pascoalino Pinheiro<sup>5</sup>  · Grayce Ellen da Cruz Paiva Lima<sup>1,2,3,6</sup>  · Camila Lopes do Amaral<sup>1,2,3</sup>  · Victor Rezende Veras<sup>1,2</sup>  · Mayara Ponte Madeira<sup>1,2,3,7</sup>  · Erika Bastos Lima Freire<sup>1,2,3,7</sup>  · Renan Galvão Ozório<sup>1,2</sup>  · Virgínia Oliveira Fernandes<sup>1,2,3,8</sup>  · Ana Paula Dias Rangel Montenegro<sup>1</sup>  · Raquel Carvalho Montenegro<sup>2</sup>  · Jeová Keny Baima Colares<sup>3</sup>  · Renan Magalhães Montenegro Júnior<sup>1,2,3,8</sup> 

José Edvar Monteiro Júnior  
edvarjunior1@gmail.com

Daniel Pascoalino Pinheiro  
danielpascoalino@gmail.com

Grayce Ellen da Cruz Paiva Lima  
grayceellen@yahoo.com.br

Camila Lopes do Amaral  
camilalamaral@gmail.com

Victor Rezende Veras  
rezende\_veras@hotmail.com

Mayara Ponte Madeira  
mayara.madeira@hotmail.com

Erika Bastos Lima Freire  
erikaendocrinologia@gmail.com

Renan Galvão Ozório  
nan.ozorio@hotmail.com

Virgínia Oliveira Fernandes  
virginiafernande@hotmail.com

Ana Paula Dias Rangel Montenegro  
apdrmontenegro@gmail.com

Raquel Carvalho Montenegro  
rcm.montenegro@gmail.com

Jeová Keny Baima Colares  
kenycolares@gmail.com

Renan Magalhães Montenegro Júnior  
renanmmjr@gmail.com

<sup>1</sup> Clinical Research Unit, Walter Cantídio University Hospital, Federal University of Ceará, Fortaleza, Brazil

<sup>2</sup> Department of Clinical Medicine, Federal University of Ceará, Fortaleza, Brazil

<sup>3</sup> PostGraduate Program in Medical Sciences, University of Fortaleza, Fortaleza, CE, Brazil

<sup>4</sup> Biology Department, Federal University of Ceará, Fortaleza, Brazil

<sup>5</sup> Department of Physiology and Pharmacology, Federal University of Ceará, Fortaleza, Brazil

<sup>6</sup> Health Sciences Center, University of Fortaleza, Fortaleza, Brazil

<sup>7</sup> Health Sciences Center, Christus University Center, Fortaleza, Brazil

<sup>8</sup> Department of Community Health, Federal University of Ceará, Fortaleza, Brazil